JCTC Journal of Chemical Theory and Computation

Nonlinearity of the Bifunctional of the Nonadditive Kinetic Energy: Numerical Consequences in Orbital-Free Embedding Calculations

Marcin Dułak and Tomasz A. Wesołowski*

Département de Chimie Physique, Université de Genève, 30, quai Ernest-Ansermet, CH-1211 Genève 4, Switzerland

Received July 24, 2006

Abstract: The bifunctional of the nonadditive kinetic energy in the reference system of noninteracting electrons ($T_s^{nad}[\rho_A, \rho_B] = T_s[\rho_A + \rho_B] - T_s[\rho_A] - T_s[\rho_B]$) is the key quantity in orbital-free embedding calculations because they hinge on approximations to $T_s^{nad}[\rho_A,\rho_B]$. Since $T_s^{nad}[\rho_A,\rho_B]$ is not linear in ρ_A, the associated potential (functional derivative) $\delta T_s^{nad}[\rho,\rho_B]/\delta\rho|_{\rho=\rho_A}(\vec{r})$ changes if ρ_A varies. In this work, for two approximations to $T_s^{nad}[\rho_A,\rho_B]$, which are nonlinear in ρ_A (gradient-free and gradient-dependent), their linearized versions are constructed, and the resulting changes (*linearization errors*) in various properties of embedded systems (orbital energies, dipole moments, interaction energies, and electron densities) are analyzed. The considered model embedded systems represent typical nonbonding interactions: van der Waals contacts, hydrogen bonds, complexes involving charged species, and intermolecular complexes of the charge-transfer character. For van der Waals and hydrogen bonded complexes, the linearization of $T_s^{nad}[\rho_A,\rho_B]$ affects negligibly the calculated properties. Even for complexes, for which large complexation induced changes of the electron density can be expected, such as the water molecule in the field of a cation, the linearization errors are about 2 orders of magnitude smaller than the interaction induced shifts of the corresponding properties. Linearization of $T_s^{nad}[\rho_A,\rho_B]$ is shown to be inadequate for the complexes of a strong charge-transfer character. Compared to gradient-free approximation to $T_s^{nad}[\rho_A,\rho_B]$, introduction of gradients increases the linearization error.

Introduction

The key quantity in orbital-free embedding calculations,[1] in which the subsystem of primary interest (*subsystem A*) is described at the orbital-level, whereas the environment of this subsystem is described using only its electron density (ρ_B), is the bifunctional of the nonadditive kinetic energy

$$T_s^{nad}[\rho_A,\rho_B] = T_s[\rho_A + \rho_B] - T_s[\rho_A] - T_s[\rho_B] \qquad (1)$$

where $T_s[\rho]$ denotes the kinetic energy in the reference system of noninteracting electrons as defined in the Levy's constrained search.[2]

The functional derivative of $T_s^{nad}[\rho_A,\rho_B]$ with respect to ρ_A is a component of the effective potential in Kohn−Sham-like one-electron equations[1] for embedded orbitals (ϕ_i^A), which are used to construct the embedded electron density ($\rho_A = 2\sum_{i=1}^{N^A}|\phi_i^A|^2$)

$$\left[-\frac{1}{2}\nabla^2 + V_{eff}^{KSCED}[\rho_A,\rho_B;\vec{r}]\right]\phi^A{}_i = \epsilon^A{}_i\phi^A{}_i \quad i = 1, N^A \qquad (2)$$

where $2N^A$ is the number of electrons in the embedded subsystem. The label KSCED stands for Kohn−Sham Equations with Constrained Electron Density and is used here to indicate that ($\{\phi_i^A\}$) are not the Kohn−Sham orbitals[3] and that the effective multiplicative potential in these equations is not the corresponding Kohn−Sham effective potential for neither the whole system nor the isolated subsystem A

* Corresponding author e-mail: tomasz.wesolowski@chiphy.unige.ch.

10.1021/ct600241q CCC: $33.50
Published on Web 10/19/2006

($V^{KS}[\rho_A;\vec{r}]$). All formulas are given in atomic units for the closed-shell case in this work. These units are also used in the discussion of numerical results except for dipole moments (in Debye, 1 D = 0.39343 e·Bohr) and orbital energies (in eV, 1 eV = 0.00367493 Hartree).

The effective potential in eq 2 has the following form

$$V_{eff}^{KSCED}[\rho_A,\rho_B;\vec{r}] = V_{eff}^{KS}[\rho_A;\vec{r}] + V_{eff}^{emb}[\rho_A,\rho_B;\vec{r}], \quad (3)$$

where the part representing the environment reads

$$V_{eff}^{emb}[\rho_A,\rho_B;\vec{r}] = \sum_{i_B}^{N_{nuc}{}^B} -\frac{Z_{i_B}}{|\vec{r}-\vec{R}_{i_B}|} + \int \frac{\rho_B(\vec{r}')}{|\vec{r}'-\vec{r}|}d\vec{r}' + \frac{\delta E_{xc}[\rho]}{\delta\rho}\Big|_{\rho=\rho_A+\rho_B} - \frac{\delta E_{xc}[\rho]}{\delta\rho}\Big|_{\rho=\rho_A} + \frac{\delta T_s^{nad}[\rho,\rho_B]}{\delta\rho}\Big|_{\rho=\rho_A} \quad (4)$$

Various computational studies based on eq 2 have been reported recently.[4−11] The functional derivative of $T_s^{nad}[\rho_A,\rho_B]$ is also used in the Cortona's formulation of density functional theory (DFT)[12] as well as in the wave function-in-DFT embedding approach by Carter, Wang, and collaborators.[13]

In the context of embedding, it is worthwhile to underline the qualitative difference between the electrostatic components (the first two terms) and the last three terms of the embedding potential in eq 4. The electrostatic components correspond to functionals which are linear in ρ_A. (The functional $F[f]$ is linear if $F[\alpha p + \beta q] = \alpha F[p] + \beta F[q]$.) The terms depending on exchange-correlation- and kinetic energies, however, correspond to functionals which are not linear in ρ_A. For a recent discussion of deviation from linearity of the exact functional $T[\rho]$, which lies at the origin of nonlinearity of $T_s^{nad}[\rho_A,\rho_B]$, see refs14 and 15 for instance. The common approximations to $T[\rho]$ also lead to such an analytic expression for $T_s^{nad}[\rho_A,\rho_B]$, which is nonlinear in ρ_A. For instance, the regular gradient expansion truncated to zeroth order (Thomas-Fermi functional,[16,17] known also as the local density approximation (LDA)), leads to the following expression

$$\tilde{T}_s^{nad(LDA)}[\rho_A,\rho_B] = (3/10)(3\pi^2)^{2/3}\int((\rho_A+\rho_B)^{5/3} - \rho_A{}^{5/3} - \rho_B{}^{5/3})d\vec{r} \quad (5)$$

which is obviously nonlinear in ρ_A. Similarly, using the generalized gradient approximation (GGA) to $T_s[\rho]$

$$T_s^{GGA}[\rho] = (3/10)(3\pi^2)^{2/3}\int \rho^{5/3}(\vec{r})F(s(\vec{r}))d\vec{r}$$

where $s = |\nabla\rho|/(2\rho k_F)$ with $k_F = (3\pi^2\rho)^{1/3}$, and $F(s)$ is an analytic function of s which might originate from various types of considerations, leads to an analytic expression for $T_s^{nad}[\rho_A,\rho_B]$ which is also nonlinear in ρ_A:

$$\tilde{T}_s^{nad(GGA)}[\rho_A,\rho_B] = (3/10)(3\pi^2)^{2/3}\int((\rho_A+\rho_B)^{5/3}F(s_{AB}) - \rho_A{}^{5/3}F(s_A) - \rho_B{}^{5/3}F(s_B))d\vec{r} \quad (6)$$

As a result, in any practical calculations the associated effective potential ($\delta T_s^{nad}[\rho_A,\rho_B]/\delta\rho_A$) changes, if ρ_A varies. From the practical point of view, it would be desirable to replace the ρ_A-dependent potential by a quantity which is not ρ_A-dependent. Such a simplification would make it possible to avoid updating the relevant component of the embedding potential during the self-consistent cycle and/or in cases where the geometry of the embedded subsystem changes. Neglecting such changes has been recognized in ref 13 as a possible additional approximation to the embedding potential of the eq 4 form.

Linearizing $T_s^{nad}[\rho_A,\rho_B]$ in ρ_A around some reference ($\rho_A{}^0$) provides a way to eliminate the dependency of $\delta T_s^{nad}[\rho,\rho_B]/\delta\rho|_{\rho=\rho_A}(\vec{r})$ on ρ_A:

$$T_s^{nad}[\rho_A,\rho_B] \approx T_s^{nad}[\rho_A{}^0,\rho_B] + \int \frac{\delta T_s^{nad}[\rho,\rho_B]}{\delta\rho}\Big|_{\rho=\rho_A{}^0}(\vec{r})(\rho_A - \rho_A{}^0)d\vec{r}. \quad (7)$$

$\rho_A{}^0$ can be chosen to be the electron density of the isolated subsystem A.

The potential corresponding to the linearized $T_s^{nad}[\rho_A,\rho_B]$ reads

$$\frac{\delta T_s^{nad}[\rho,\rho_B]}{\delta\rho}\Big|_{\rho=\rho_A}(\vec{r}) \approx \frac{\delta T_s^{nad}[\rho,\rho_B]}{\delta\rho}\Big|_{\rho=\rho_A{}^0}(\vec{r}) \quad (8)$$

The approximation of eq 8 applied in eq 2 affects obviously the embedded orbitals. As a consequence, molecular properties are affected by this approximation. For any observable, the difference between the results obtained from the linearized and nonlinearized versions of eq 2 are referred to as *linearization error* (LE) in this work. The approximation of eq 8 is referred to as *linearization approximation*. $\rho_A{}^0$ and ρ_B are chosen as the Kohn−Sham ground-state electron densities of the isolated subsystems A and B. The local density approximation[18−20] to the exchange-correlation energy functional ($E_{xc}[\rho]$) is used in all calculations.

The set of model embedded subsystems considered here (see Table 1) comprises molecules involved in common nonbonding interactions occurring in soft-condensed matter: van der Waals contacts, hydrogen bonded complexes, complexes involving charged species, and a representative intermolecular complex of a charge-transfer character.[21] They form a series, in which formation of the complex involves electron density deformation of increasing magnitude. In particular, the electron density deformation in the NH_3−ClF complex is known to be strong.[21] The adequacy of the *linearization approximation*, in which the electron density of the isolated molecule is used as $\rho_A{}^0$ in eq 11, can be expected to decrease along this series. Note that homomolecular dimers occur twice in the tables because the two monomers are not equivalent.

The *linearization errors* of the following complexation induced properties: energies of interactions between the subsystems, dipole moments, orbital energies, and deformations of electron density are analyzed.

Unless specified, the discussed results are obtained using the aug-cc-pVTZ[22,23] basis set for all elements except for lithium (cc-pVTZ[24,23]). The atomic basis sets are centered on all atoms in the whole investigated complex including

Table 1: Errors in Orbital Energies ($\delta\Delta\epsilon^A$) Arising from the Linearization of $\tilde{T}_s^{nad(GGA97)}[\rho_A,\rho_B]$ for the Highest Occupied Embedded Orbital (HOEO) and the Lowest Unoccupied Embedded Orbital (LUEO)[c]

subsystem					
A	B	$\delta\Delta\epsilon_{HOEO}{}^A$	$\delta\Delta\epsilon_{LUEO}{}^A$	$\Delta\epsilon_{HOEO}{}^A$	$\Delta\epsilon_{LUEO}{}^A$
Ne	Ne	0	−0.1	−10.9	−42.8
CH_4	CH_4	0.1	1.5	−2.1	−293.8
CH_4	CH_4	0.1	1.5	−2.1	−293.8
C_2H_2	C_2H_2	0.4	2.9	−58.1	−169.9
C_2H_2	C_2H_2	0.4	2.9	−58.1	−169.9
H_2O	H_2O[a]	−1.5	−2.2	508.6	168.4
H_2O[a]	H_2O	3.9	1.9	−644.9	−252.9
NH_3[a]	H_2O	7.0	1.9	−746.4	−223.0
H_2O	NH_3[a]	−2.2	−2.8	710.6	134.0
HF[a]	HF	3.6	3.3	−1037.7	−506.6
HF	HF[a]	−1.2	−2.1	361.5	141.5
NH_3	ClF	183.7	596.0	−1253.7	−1129.2
ClF	NH_3	−3.2	−19.0	817.1	1207.9
Li^+	H_2O	−0.5	0.6	1449.2	270.4
H_2O	Li^+	23.3	112.7	−7127.2	−6547.8

[a] Acceptor of the hydrogen bond. [b] Geometries of the complexes taken from refs 26 and 4 for Li^+-H_2O. [c] The complexation induced shifts of HOEO ($\Delta\epsilon_{HOEO}{}^A$) and LUEO ($\Delta\epsilon_{LUEO}{}^A$) are given for reference. All values in meV.

Table 2: Errors in Orbital Energies ($\delta\Delta\epsilon^A$) Arising from the Linearization of $\tilde{T}_s^{nad(LDA)}[\rho_A,\rho_B]$ for the Highest Occupied Embedded Orbital (HOEO) and the Lowest Unoccupied Embedded Orbital (LUEO)[c]

subsystem					
A	B	$\delta\Delta\epsilon_{HOEO}{}^A$	$\delta\Delta\epsilon_{LUEO}{}^A$	$\Delta\epsilon_{HOEO}{}^A$	$\Delta\epsilon_{LUEO}{}^A$
Ne	Ne	0	0	−2.9	82.2
CH_4	CH_4	0	0.7	16.6	−252.0
CH_4	CH_4	0	0.7	16.6	−252.0
C_2H_2	C_2H_2	0.2	1.9	−39.4	−143.7
C_2H_2	C_2H_2	0.2	1.9	−39.4	−143.7
H_2O	H_2O[a]	−2.9	−3.7	551.4	216.4
H_2O[a]	H_2O	3.5	1.4	−589.1	−220.0
NH_3[a]	H_2O	6.0	1.1	−669.8	−196.6
H_2O	NH_3[a]	−4.1	−4.2	756.5	174.1
HF[a]	HF	3.8	2.7	−993.4	−468.8
HF	HF[a]	−2.4	−4.3	410.2	212.5
NH_3	ClF	89.8	173.6	−979.7	−603.7
ClF	NH_3	−6.3	−25.0	884.3	1333.5
Li^+	H_2O	−1.8	−0.8	1535.4	398.8
H_2O	Li^+	20.4	82.9	−7077.2	−6568.9

[a] Acceptor of the hydrogen bond. [b] Geometries of the complexes taken from refs 26 and 4 for Li^+-H_2O. [c] The complexation induced shifts of HOEO ($\Delta\epsilon_{HOEO}{}^A$) and LUEO ($\Delta\epsilon_{LUEO}{}^A$) are given for reference. All values in meV.

the embedded subsystem and its environment (KSCED(s) calculations according to the nomenclature of ref 25) for equilibrium geometries of each dimer.[26] In a dedicated section concerning the role of the size of the atomic basis sets on the evaluated errors the following series of basis sets is used: aug-cc-pVDZ, aug-cc-pVTZ, aug-cc-pVQZ, and aug-cc-pV5Z.[22,23] Additionally, errors due to linearization of $T_s^{nad}[\rho_A,\rho_B]$ in ρ_A have been analyzed for exchange-correlation energy functional of the GGA type (Perdew and Wang[27,28]). All the calculations are performed on the "(99,590)p" pruned grid using 10^{-9} self-consistent cycle convergence criterion and the GEN-A4* auxiliary basis set.[29]

Two levels of approximation to $T_s^{nad}[\rho_A,\rho_B]$ and the associated functional derivative are considered: (a) local density approximation $\tilde{T}_s^{nad(LDA)}[\rho_A,\rho_B]$[1], defined in eq 8, and (b) $\tilde{T}_s^{nad(GGA97)}[\rho_A,\rho_B]$[25], defined in eq 9, in which the function $F(s)$ has the Lembarki-Chermette (LC94) form[30]

$$F^{LC94}(s) = \frac{1 + 0.093907s\,\mathrm{arcsinh}(76.32s) + (0.26608 - 0.0809615e^{-100s2})s^2}{1 + 0.093907s\,\mathrm{arcsinh}(76.32s) + 0.57767 \cdot 10^{-4}s^4}$$

Tildas used above indicate that the considered functionals are not exact.

The GGA97 approximation to $T_s^{nad}[\rho_A,\rho_B]$ is considered here in addition to $\tilde{T}_s^{nad(LDA)}[\rho_A,\rho_B]$ because of its use in most of our own studies applying eq 2 for embedded subsystems where ρ_A and ρ_B do not overlap strongly. The GGA97 choice is motivated by the fact that the associated functional derivative was shown to be the most accurate among several gradient-dependent approximations[25,31] in the case of small overlaps between ρ_A and ρ_B.

Results and Discussions

Orbital Energies. Table 1 collects the linearization errors in the energies of the highest occupied (HOEO) and lowest unoccupied embedded orbitals (LUEO) in the $\tilde{T}_s^{nad(GGA97)}[\rho_A,\rho_B]$ case. For molecules involved in van der Waals complexes or hydrogen bonds, LE in orbital energies is so small (meV range) that it can be neglected in almost any discussion of chemical relevance. Typically, LEs are 2 orders of magnitude smaller than the complexation induced shifts of orbital energies. The complexation induced shift of the orbital energy for the subsystem A ($\Delta\epsilon^A$) is defined as the difference between the energies of the corresponding orbitals in the embedded- and free subsystem A ($\Delta\epsilon^A = \epsilon^A - \epsilon^{A0}$). For H_2O in Li^+-H_2O, numerical values of LE are significantly larger (0.1 eV range); they are, however, still about 2 orders of magnitude smaller than the total complexation induced shifts of this property. Such small relative errors in this case might even seem surprising, taking into account the fact that the cation polarizes strongly the water molecule in the complex and the adequacy of using $\rho_A{}^0$ in eq 8 is not evident. LEs amount to less than 10% of the complexation induced shifts in the orbital energies in this case. For NH_3 in the NH_3-ClF complex, however, LE in the energy of LUEO reaches 0.6 eV which is unacceptable because this error represents about 50% of the magnitude of complexation induced shifts of HOEO or LUEO. This failure of the *linearization approximation* of eq 8 could be expected because the NH_3-ClF complex is known for its charge-transfer character.[21]

It is worthwhile to notice that LEs in the energies of unoccupied orbitals are larger than the ones of occupied orbitals in almost all cases. The fact that *linearization approximation* affects more unoccupied orbitals than occupied ones, indicates that linearizing $\tilde{T}_s^{nad}[\rho_A,\rho_B]$ should be applied with a proper care in such applications of the orbital-free embedding potential which aim at the energies of the electronic excitations.[32,33]

Table 3: Relative Errors in the Interaction Energy ($\delta E_{int}^{A}/E_{int}^{A}$ in ‰), Arising from the Linearization of $\tilde{T}_s^{nad(GGA97)}[\rho_A,\rho_B]$ and $\tilde{T}_s^{nad(LDA)}[\rho_A,\rho_B]$[c]

subsystem		GGA97		LDA	
A	B	$\delta E_{int}^{A}/E_{int}^{A}$	E_{int}^{A}	$\delta E_{int}^{A}/E_{int}^{A}$	E_{int}^{A}
Ne	Ne	0	−518	0	−130
CH_4	CH_4	0	−2524	0	−683
CH_4	CH_4	0	−2524	−0.01	−683
C_2H_2	C_2H_2	−0.01	−4521	−0.01	−2445
C_2H_2	C_2H_2	−0.01	−4521	−0.01	−2445
H_2O	H_2O[a]	−0.04	−11487	−0.11	−6492
H_2O[a]	H_2O	−0.09	−11620	−0.10	−6012
NH_3[a]	H_2O	−0.15	−14662	−0.14	−8053
H_2O	NH_3[a]	−0.05	−14530	−0.15	−8672
HF[a]	HF	−0.14	−10142	−0.19	−5112
HF	HF[a]	−0.02	−9010	−0.08	−4558
NH_3	ClF	−28.18	−23024	−122.35	−1423
ClF	NH_3	−0.25	−19437	−6.42	−1003
Li^+	H_2O	0	−46752	0	−41423
H_2O	Li^+	−0.41	−72880	−0.31	−65132

[a] Acceptor of the hydrogen bond. [b] Geometries of the complexes taken from refs 26 and 4 for Li^+-H_2O. [c] The interaction energies (E_{int}^{A} in μHartree) are given for reference.

Usually, LEs in orbital energies are smaller for $\tilde{T}_s^{nad(LDA)}[\rho_A,\rho_B]$ than for $\tilde{T}_s^{nad(GGA97)}[\rho_A,\rho_B]$ (compare Tables 1 and 2).

Interaction Energies. Once the embedded orbitals ($\{\phi_i^A\}$) are obtained from eq 2, the interaction energy between subsystem A and its environment (subsystem B) reads

$$\begin{aligned} E_{int}^{A} &= E^{s}[\{\phi_i^A\},\rho_B] - E^{KS}[\rho_A^0] - E^{KS}[\rho_B] \\ &= V[\rho_A+\rho_B] + J[\rho_A+\rho_B] + E_{xc}[\rho_A+\rho_B] \\ &\quad + T_s^{nad}[\rho_A,\rho_B] + 2\sum_{i=1}^{N^A}\left\langle \phi_i^A\left| -\frac{1}{2}\nabla^2 \right|\phi_i^A\right\rangle + T_s[\rho_B] \\ &\quad + E_{NN}^{AB} - E^{KS}[\rho_A^0] - E^{KS}[\rho_B] \quad (9) \end{aligned}$$

where $E^{KS}[\rho_A^0]$ and $E^{KS}[\rho_B]$ denote the Kohn−Sham energy functionals for isolated subsystems A and B, whereas E_{NN}^{AB} is the energy of repulsion between nuclei in the total system, $V[\rho_A+\rho_B]$ is the functional of the nuclear attraction energy (total), and $J[\rho_A+\rho_B]$ is the functional of the electron−electron Coulomb repulsion (total). Note that in the numerical evaluation of E_{int}^{A}, some components of the energy are not calculated at all because they cancel each other (for instance the kinetic energy contribution T_s to $E^{KS}[\rho_B]$ cancels the $T_s[\rho_B]$ term).

Table 3 collects the linearization errors in the energy of interaction between the embedded subsystem and its environment for $\tilde{T}_s^{nad(GGA97)}[\rho_A,\rho_B]$ and $\tilde{T}_s^{nad(LDA)}[\rho_A,\rho_B]$. Linearization of $\tilde{T}_s^{nad}[\rho_A,\rho_B]$ is very adequate as it affects the interaction energies by a small amount (range of μHartrees) in all cases except for the charge-transfer complex where it reaches 649 μHartree (for the GGA97 functional). As discussed previously, the charge-transfer case lies outside of the domain of applicability of the *linearization approximation*. Among other systems, the largest LE occurs for water interacting with Li^+ where it reaches 30 μHartree (again for the GGA97 functional). The GGA97 interaction energies are larger in absolute values than the LDA ones, and the effect of linearization of $\tilde{T}_s^{nad(GGA97)}[\rho_A,\rho_B]$ is systematically slightly larger than it is for $\tilde{T}_s^{nad(LDA)}[\rho_A,\rho_B]$.

Table 4: Errors in the Complexation Induced Dipole Moments ($\delta\Delta\mu^A$), Arising from the Linearization of $\tilde{T}_s^{nad(GGA97)}[\rho_A,\rho_B]$[c]

subsystem							
A	B	$\delta\Delta\mu_x^A$	$\delta\Delta\mu_y^A$	$\delta\Delta\mu_z^A$	$\Delta\mu_x^A$	$\Delta\mu_y^A$	$\Delta\mu_z^A$
Ne	Ne	0	0	0	0	0	5.0
Ne	Ne	0	0	0	0	0	−5.0
CH_4	CH_4	0	0	−0.3	0	0	30.7
CH_4	CH_4	0	0	0.3	0	0	−30.7
C_2H_2	C_2H_2	0.4	−1.0	0	−122.0	55.1	0
C_2H_2	C_2H_2	−0.4	1.0	0	122.0	−55.1	0
H_2O	H_2O[a]	2.5	0	−0.2	−209.7	−3.2	41.5
H_2O[a]	H_2O	4.3	0	0.2	−258.4	4.7	−64.8
NH_3[a]	H_2O	7.9	−0.6	0	−337.1	75.0	0.3
H_2O	NH_3[a]	3.7	0.2	0	−289.5	−19.3	−0.1
HF[a]	HF	−4.0	−0.3	0	276.0	58.9	0
HF	HF[a]	−1.3	0.1	0	101.9	−37.0	0
NH_3	ClF	0	0	287.6	0	0	−983.1
ClF	NH_3	0	0	12.4	0	0	−675.1
Li^+	H_2O	0	0	0	0	0	−13.1
H_2O	Li^+	0	0	32.5	0	0	−1657.0

[a] Acceptor of the hydrogen bond. [b] Geometries of the complexes taken from refs 26 and 4 for Li^+-H_2O. [c] The total complexation induced dipole moments ($\Delta\mu^A$) are given for reference. All values in mDebye.

For practical purposes, it is important that LE in energy does not vary with the changing geometry. To this end, LEs were analyzed along the LDA dissociation energy curve for Li^+-H_2O. As indicated in previous sections the *linearization approximation* is still applicable for Li^+-H_2O despite the strong polarization of water due to the electric field of the cation. A larger basis set (aug-cc-pVQZ for O and H, and cc-pVQZ for Li) than the one used in calculations discussed so far and $\tilde{T}_s^{nad(LDA)}[\rho_A,\rho_B]$ were applied. LE remain small in the whole range of intermolecular distances. At an equilibrium intermolecular distance of 1.80 Å, LE in the interaction energy amounts to 25 μHartree, and it does not exceed 80 μHartree even at intermolecular distances as short as 0.7 Å. LEs are decreasing with increasing intermolecular distance, which reflects the fact that the exact $T_s^{nad}[\rho_A,\rho_B]$ functional disappears for nonoverlapping ρ_A and ρ_B, and this asymptotic condition is satisfied also by $\tilde{T}_s^{nad(LDA)}[\rho_A,\rho_B]$ and $\tilde{T}_s^{nad(GGA97)}[\rho_A,\rho_B]$ considered in this work. Therefore, the contribution of the kinetic energy terms decreases with increasing intersystem distance.

Dipole Moments. The *linearization errors* in dipole moments are collected in Tables 4 and 5. Except for the charge-transfer complex, linearization of $\tilde{T}_s^{nad}[\rho_A,\rho_B]$ is very adequate in all embedded systems. For $\tilde{T}_s^{nad(LDA)}[\rho_A,\rho_B]$, LEs in dipole moments are small and do not exceed 6% of the total complexation induced dipole moments. Opposite, to the previously analyzed observables, the complexation induced dipole moments depend strongly on the choice of the approximation for $T_s^{nad}[\rho_A,\rho_B]$.

Complexation Induced Density Deformations. Orbital energies, interaction energies, and dipole moments are global

Table 5: Errors in the Complexation Induced Dipole Moments ($\delta\Delta\mu^A$), Arising from the Linearization of $\tilde{T}_s^{nad(LDA)}[\rho_A,\rho_B]^c$

subsystem							
A	B	$\delta\Delta\mu_x{}^A$	$\delta\Delta\mu_y{}^A$	$\delta\Delta\mu_z{}^A$	$\Delta\mu_x{}^A$	$\Delta\mu_y{}^A$	$\Delta\mu_z{}^A$
Ne	Ne	0	0	0	0	0	0.7
Ne	Ne	0	0	0	0	0	−0.7
CH_4	CH_4	0	0	0	0	0	−6.3
CH_4	CH_4	0	0	0	0	0	6.3
C_2H_2	C_2H_2	0.4	−0.6	0	−117.2	10.9	0
C_2H_2	C_2H_2	−0.4	0.6	0	117.2	−10.9	0
H_2O	H_2O^a	4.3	0	−0.4	−262.7	−3.3	43.9
H_2O^a	H_2O	3.8	0	0.3	−206.4	4.6	−65.4
$NH_3{}^a$	H_2O	6.3	−0.6	0	−264.9	72.3	0.3
H_2O	$NH_3{}^a$	6.1	0.4	0	−344.1	−21.6	−0.1
HF^a	HF	−3.9	−0.3	0	238.1	58.1	0.0
HF	HF^a	−2.5	0.2	0	145.9	−38.0	0.1
NH_3	ClF	0	0	134.2	0	0	−675.8
ClF	NH_3	0	0	18.1	0	0	−795.8
Li^+	H_2O	0	0	0.2	0	0	−19.7
H_2O	Li^+	0	0	27.9	0	0	−1596.0

[a] Acceptor of the hydrogen bond. [b] Geometries of the complexes taken from refs 26 and 4 for Li^+-H_2O. [c] The total complexation induced dipole moments ($\Delta\mu^A$) are given for reference. All values in mDebye.

quantities for the embedded system. Any change in the effective potential such as linearization of $T_s^{nad}[\rho_A,\rho_B]$ might affect them less than local quantities such as electron density perturbation: $\Delta\rho_A = \rho_A - \rho_A{}^0$. Analyses made in previous sections indicate that Li^+-H_2O is the one among the analyzed systems, for which LEs are the largest being sufficiently small that the *linearization approximation* is fully applicable. For this system, large changes of electron density can be expected due to the polarization of the water molecule (subsystem A) by the positive charge of the cation. Indeed, electron density deformation derived from conventional Kohn−Sham calculations is the largest in the vicinity of the oxygen atom (see Figure 1). The embedding calculations, without linearization of $\tilde{T}_s^{nad(LDA)}[\rho_A,\rho_B]$ lead to electron density deformation which follows closely the Kohn−Sham trends. It indicates that $\delta\tilde{T}_s^{nad(LDA)}[\rho,\rho_B]/\delta\rho|_{\rho=\rho_A}(\vec{r})$ is a very good approximation to the exact potential $\delta T_s^{nad}[\rho,\rho_B]/\delta\rho|_{\rho=\rho_A}(\vec{r})$. Interestingly, linearization of $\tilde{T}_s^{nad(LDA)}[\rho_A,\rho_B](\vec{r})$ does not lead to any noticeable effect on complexation induced density deformations. LE is so small in this case that it is almost not visible on the figure. In fact, the largest LEs do not exceed 5×10^{-4} eÅ^{-3}, i.e., are between 1 or 2 orders of magnitude smaller than the complexation induced density deformations.

It is worthwhile to notice that LEs are much smaller than the errors of $\delta\tilde{T}_s^{nad(LDA)}[\rho,\rho_B]/\delta\rho|_{\rho=\rho_A}(\vec{r})$ which are responsible for the deviations from the reference Kohn−Sham data.

Nonlinearity of $T_s^{nad}[\rho_A,\rho_B]$: The Effect of Changing the Basis Sets and Approximations for $E_{xc}[\rho]$. Increasing the flexibility of the used basis sets and changing the approximation for the exchange-correlation energy functional provides another possibility to detect flaws of the *linearization approximation* of eq 8. Similar analyses as the ones discussed in the previous sections are made here using a series of atomic basis sets of increasing completeness starting from aug-cc-pVDZ until aug-cc-pV5Z. Five representative embedded systems for which previous calculations indicate the adequacy of the linearization of $T_s^{nad(LDA)}[\rho_A,\rho_B]$ are chosen for this analysis: (i) Ne in the Ne_2 dimer, (ii) HF (donor of the hydrogen bond) in the $(HF)_2$ dimer, (iii) HF (acceptor of the hydrogen bond) in the $(HF)_2$ dimer, (iv) H_2O (donor of the hydrogen bond) in the $(H_2O)_2$ dimer, and (v) H_2O (acceptor of the hydrogen bond) in the $(H_2O)_2$ dimer.

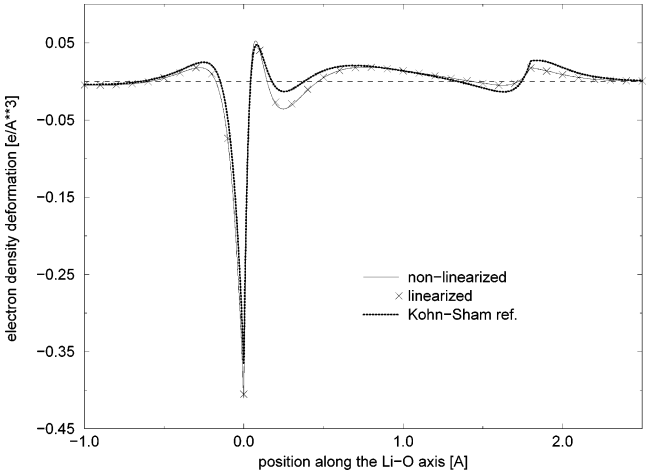

Figure 1. Complexation induced deformation of the electron density of H_2O in Li^+-H_2O calculated using linearized and nonlinearized $\tilde{T}_{snad(LDA)}[\rho_A,\rho_B]$. The oxygen atom is situated at $z = 0.0$ Å and the lithium at $z = 1.8$ Å. The deformation of the total electron density derived from the LDA Kohn−Sham calculations is given for reference.

LEs in the interaction energy are lower or equal than 1 μHartree for all five systems, using all the basis sets. As far as LEs in the orbital energies are concerned, they lie well below the 5 meV threshold. It is worthwhile to note that such small errors are negligible compared to the variability of the complexation induced shifts in the orbital energies calculated using various basis sets.

The negligible variation of LEs of all investigated properties upon the changes of the basis set results probably from the fact that embedded orbitals are constructed using *all* atomic centers including the atoms of the environment. Therefore, even at the aug-cc-pVDZ level $\delta T_s^{nad}[\rho,\rho_B]/\delta\rho|_{\rho=\rho_A}(\vec{r})$ is adequately represented around atoms of the environment.

The change of approximation for the exchange-correlation energy from LDA to GGA does not influence the observed trends concerning the errors due to linearization of $T_s^{nad}[\rho_A,\rho_B]$ in ρ_A. For instance, for PW91 approximation the largest LE of the interaction energy is found for NH_3-ClF and reaches 532 μHartree (for the GGA97 functional, using the aug-cc-pVTZ basis set).

Conclusions

The linearization of $\tilde{T}_s^{nad(LDA)}[\rho_A,\rho_B]$ and $\tilde{T}_s^{nad(GGA97)}[\rho_A,\rho_B]$ using the Kohn−Sham ground-state electron density of the isolated subsystem A in eq 8 leads to negligible numerical effects on properties for all (except for the NH_3-ClF complex) studied systems. The largest linearization errors

are 2 orders of magnitude smaller than the complexation induced shifts in molecular properties in such cases. Among the analyzed properties, the energies of unoccupied orbitals are typically the most affected by the linearization of $T_s^{nad}[\rho_A,\rho_B]$ in ρ_A. Among these cases where the *linearization approximation* is adequate the largest *linearization error* occurs for the energy of the lowest unoccupied embedded orbital in the case of the water molecule in the Li^+-H_2O complex. Linearization of $\tilde{T}_s^{nad(GGA97)}[\rho_A,\rho_B]$ results in the change of the orbital energy in the range of 0.1 eV which is still about 60 times smaller than the whole complexation induced energy shift of this orbital.

In the NH_3-ClF case, even larger deformations of electron density accompany the formation of the complex. For this system using the electron densities of isolated monomers to linearize $T_s^{nad}[\rho_A,\rho_B]$ was shown not to be adequate.

The linearization in ρ_A leads usually to smaller effects in the case of $\tilde{T}_s^{nad(LDA)}[\rho_A,\rho_B]$ than $\tilde{T}_s^{nad(GGA97)}[\rho_A,\rho_B]$. Since neither $\tilde{T}_s^{nad(LDA)}[\rho_A,\rho_B]$ nor $\tilde{T}_s^{nad(GGA97)}[\rho_A,\rho_B]$ are exact, this result indicates that the adequacy of linearization should be checked if intended to be applied to any new type of approximation for $T_s^{nad}[\rho_A,\rho_B]$.

Our calculations show that the linearization error does not vary significantly with changing atomic basis sets within the aug-cc-pVXZ family and that similar linearization errors are obtained using the LDA and the GGA (PW91) exchange-correlation functionals.

Acknowledgment. This work was supported by Swiss National Science Foundation.

References

(1) Wesołowski, T. A.; Warshel, A. *J. Phys. Chem.* **1993**, *97*, 8050−8053.

(2) Levy, M. *Proc. Natl. Acad. Sci. U.S.A.* **1979**, *76*, 6062−6065.

(3) Kohn, W.; Sham, L. J. *Phys. Rev.* **1965**, *140*, A1133−A1138.

(4) Stefanovich, E. V.; Truong, T. N. *J. Chem. Phys.* **1996**, *104*, 2946−2955.

(5) Mei, W. N.; Boyer, L. L.; Mehl, M. J.; Ossowski, M. M.; Stokes, H. T. *Phys. Rev. B* **2000**, *61*, 11425−11431.

(6) Trail, J. R.; Bird, D. M. *Phys. Rev. B* **2000**, *62*, 16402−16411.

(7) Shimojo, F.; Kalia, R. K.; Nakano, A.; Vashishta, P. *Comput. Phys. Commun.* **2005**, *167*, 151−164.

(8) Neugebauer, J.; Louwerse, M. J.; Baerends, E. J.; Wesołowski, T. A. *J. Chem. Phys.* **2005**, *122*, 094115.

(9) Olsson, M. H. M.; Hong, G. Y.; Warshel, A. *J. Am. Chem. Soc.* **2003**, *125*, 5025−5039.

(10) Choly, N.; Lu, G.; E, W.; Kaxiras, E. *Phys. Rev. B* **2005**, *71*, 094101.

(11) Iannuzzi, M.; Kirchner, B.; Hutter, J. *Chem. Phys. Lett.* **2006**, *421*, 16−20.

(12) Cortona, P. *Phys. Rev. B* **1991**, *44*, 8454−8458.

(13) Kluner, T.; Govind, N.; Wang, Y. A.; Carter, E. A. *J. Chem. Phys.* **2002**, *116*, 42−54.

(14) Chan, G. K. L.; Handy, N. C. *Phys. Rev. A* **1999**, *59*, 2670−2679.

(15) Gal, T. *Phys. Rev. A* **2001**, *6406*, 062503.

(16) Thomas, L. H. *Proc. Cambridge Philos. Soc.* **1927**, *23*, 542.

(17) Fermi, E. *Z. Phys.* **1928**, *48*, 73.

(18) Dirac, P. A. M. *Proc. Cambridge Philos. Soc.* **1930**, *26*, 376−385.

(19) Ceperley, D. M.; Alder, B. J. *Phys. Rev. Lett.* **1980**, *45*, 566−569.

(20) Vosko, S. H.; Wilk, L.; Nusair, M. *Can. J. Phys.* **1980**, *58*, 1200−1211.

(21) Ruiz, E.; Salahub, D. R.; Vela, A. *J. Phys. Chem.* **1996**, *100*, 12265−12276.

(22) Kendall, R. A.; Dunning, T. H.; Harrison, R. J. *J. Chem. Phys.* **1992**, *96*, 6796−6806.

(23) Basis sets were obtained from the Extensible Computational Chemistry Environment Basis Set Database, Version 02/25/04, as developed and distributed by the *Molecular Science Computing Facility, Environmental and Molecular Sciences Laboratory* which is part of the *Pacific Northwest Laboratory*, P.O. Box 999, Richland, WA 99352, U.S.A., and funded by the *U.S. Department of Energy*. The *Pacific Northwest Laboratory* is a multiprogram laboratory operated by *Battelle Memorial Institute* for the *U.S. Department of Energy* under contract DE-AC06-76RLO 1830. Contact *David Feller* or *Karen Schuchardt* for further information. http://www.emsl.pnl.gov/forms/basisform.html (accessed May 25, 2004).

(24) Dunning, T. H. *J. Chem. Phys.* **1989**, *90*, 1007−1023.

(25) Wesołowski, T. A. *J. Chem. Phys.* **1997**, *106*, 8516−8526.

(26) Zhao, Y.; Truhlar, D. G. *J. Chem. Theory Comput.* **2005**, *1*, 415−432.

(27) Perdew, J. P.; Chevary, J. A.; Vosko, S. H.; Jackson, K. A.; Pederson, M. R.; Singh, D. J.; Fiolhais, C. *Phys. Rev. B* **1992**, *46*, 6671−6687.

(28) Perdew, J. P.; Chevary, J. A.; Vosko, S. H.; Jackson, K. A.; Pederson, M. R.; Singh, D. J.; Fiolhais, C. *Phys. Rev. B* **1993**, *48*, 4978−4978.

(29) Köster, A. M.; Calaminici, P.; Escalante, S.; Flores-Moreno, R.; Goursot, A.; Patchkovskii, S.; Reveles, J. U.; Salahub, D. R.; Vela, A.; Heine, T. *The deMon User's Guide, Version 1.0.3, 2003−2004*. http://www.deMon-software.com/ (accessed Sep 8, 2006).

(30) Lembarki, A.; Chermette, H. *Phys. Rev. A* **1994**, *50*, 5328−5331.

(31) Wesołowski, T. A.; Chermette, H.; Weber, J. *J. Chem. Phys.* **1996**, *105*, 9182−9190.

(32) Casida, M. E.; Wesołowski, T. A. *Int. J. Quantum Chem.* **2004**, *96*, 577−588.

(33) Wesołowski, T. A. *J. Am. Chem. Soc.* **2004**, *126*, 11444−11445.

CT600241Q